

## Supplementary Materials for

### Protein O-GlcNAcylation Is Required for Fibroblast Growth Factor Signaling in *Drosophila*

Daniel Mariappa, Kathrin Sauert, Karina Mariño, Daniel Turnock, Ryan Webster, Daan M. F. van Aalten, Michael A. J. Ferguson, H.-Arno J. Müller\*

\*To whom correspondence should be addressed. E-mail: h.j.muller@dundee.ac.uk

Published 20 December 2011, *Sci. Signal.* **4**, ra89 (2011)  
DOI: 10.1126/scisignal.2002335

#### The PDF file includes:

- Fig. S1. Hexosamine biosynthesis pathway.
- Fig. S2. EGFR-dependent MAPK activation in the ectoderm in *nst*<sup>MZ</sup> embryos.
- Fig. S3. Molecular cloning and transgenic rescue of *nst*.
- Fig. S4. O-GlcNAc immunostaining is reduced in *nst*<sup>16923MZ</sup> embryos.
- Fig. S5. Changes in protein O-GlcNAcylation upon modulation of OGT and OGA activity in S2 cells.
- Fig. S6. Lack of mesoderm phenotype in *sxc*, *nst* double mutants.
- Table S1. Genetic interaction between *nst* and *htl*.
- Table S2. Rescue of hatching defects in *nst*<sup>MZ</sup> embryos.
- Table S3. Measurement of UDP-HexNAc in *mmv* and *nst* embryos.
- Table S4. Tissue-specific rescue of the *nst* phenotype.
- Table S5. Epistasis experiment of *nst* mutants with  $\lambda$ Htl.
- Table S6. Suppression of *nst* phenotype by GlcNAcstatin C.
- Table S7. Overexpression of O-GlcNAc-cycling enzymes in *nst* mutants.
- Table S8. Oligonucleotide primers used in this study.

## Hexosamine Biosynthetic Pathway

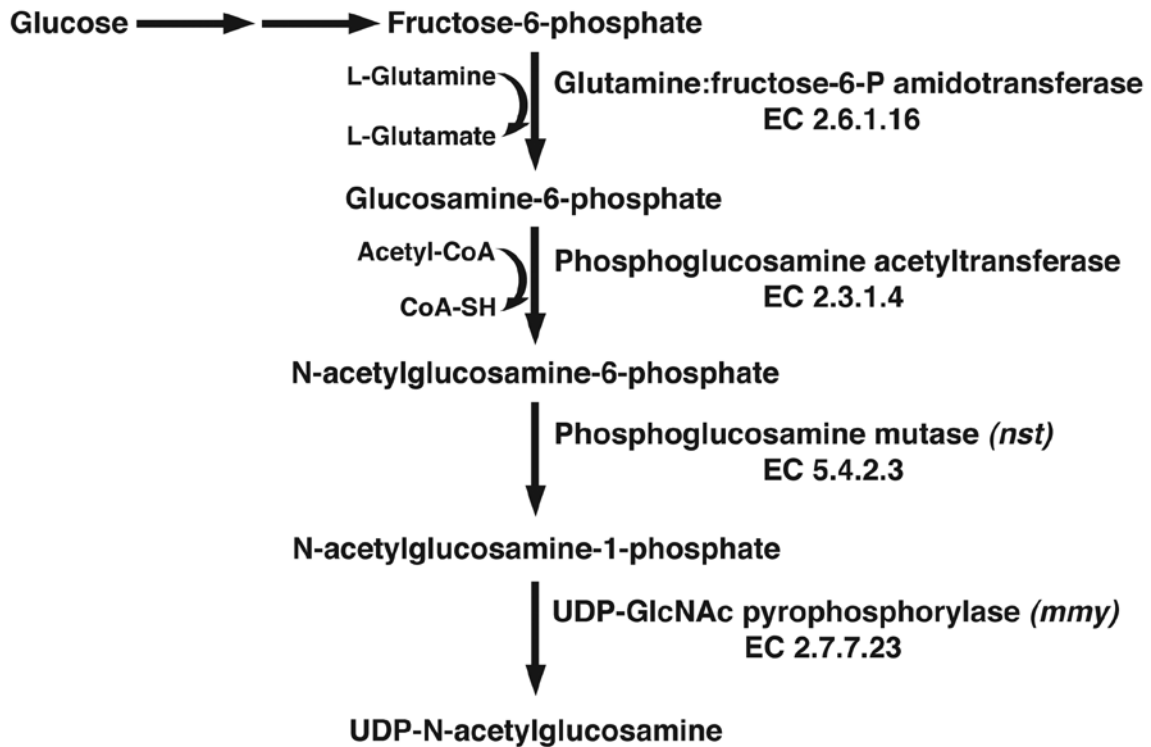


**Fig. S1. Hexosamine biosynthesis pathway.** Glucose is transported into the cytoplasm and either enters the glycolytic pathway or the glycogen biosynthesis pathway, or is converted to fructose-6-phosphate and enters the hexosamine pathway. *nst* encodes phosphoacetylglucosamine mutase (PAGM) and *mmy* encodes UDP-GlcNAc pyrophosphorylase. The enzyme classification (EC) numbers are shown for each of the enzymes.

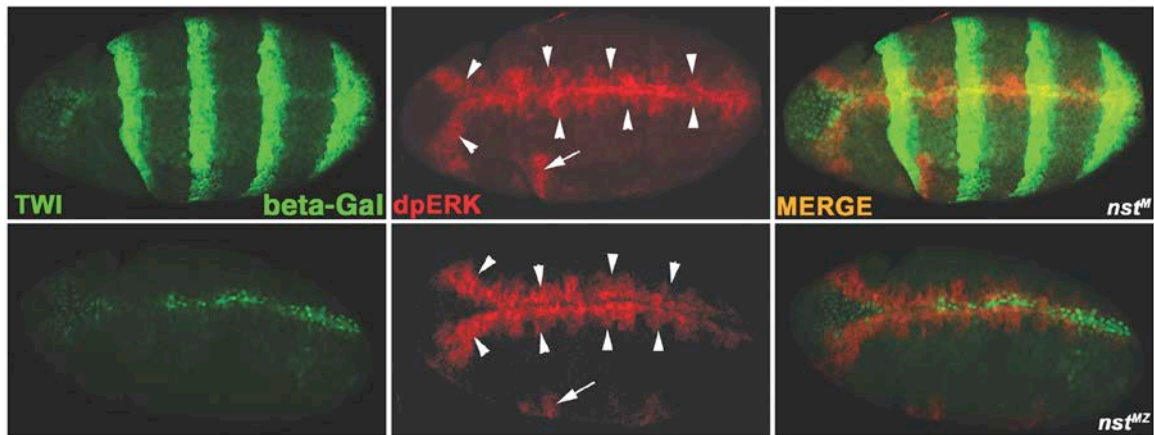


**Fig. S2. EGFR-dependent MAPK activation in the ectoderm in  $nst^{M/Z}$  embryos.** Embryos from  $nst^{16924}$  germ line clone bearing females were obtained by crossing to  $nst^{16924}/TM3[ftz::lacZ]$  males. The presence of the lacZ transgene on the *TM3* balancer chromosome was used for genotyping and detected by anti- $\beta$ -galactosidase antibodies (beta-Gal, green in upper panels, expression is marked in 4 stripes) staining. The mesoderm is marked by the presence of Twist (TWI) (green). MAPK activation is detected by immunolabeling with anti-dpERK antibody (red). The arrowheads mark the presence of activated MAPK in the ectoderm alongside the ventral midline. This activation is dependent on EGFR signaling (1) and is unimpaired in  $nst^{16923}$  M/Z mutants. Similarly, EGFR-dependent MAPK activation at the cephalic furrow (arrows) is also normal in  $nst^{16923}$  MZ.

1. L. Gabay, R. Seger, B. Z. Shilo, In situ activation pattern of Drosophila EGF receptor pathway during development. *Science* **277**, 1103-1106 (1997).

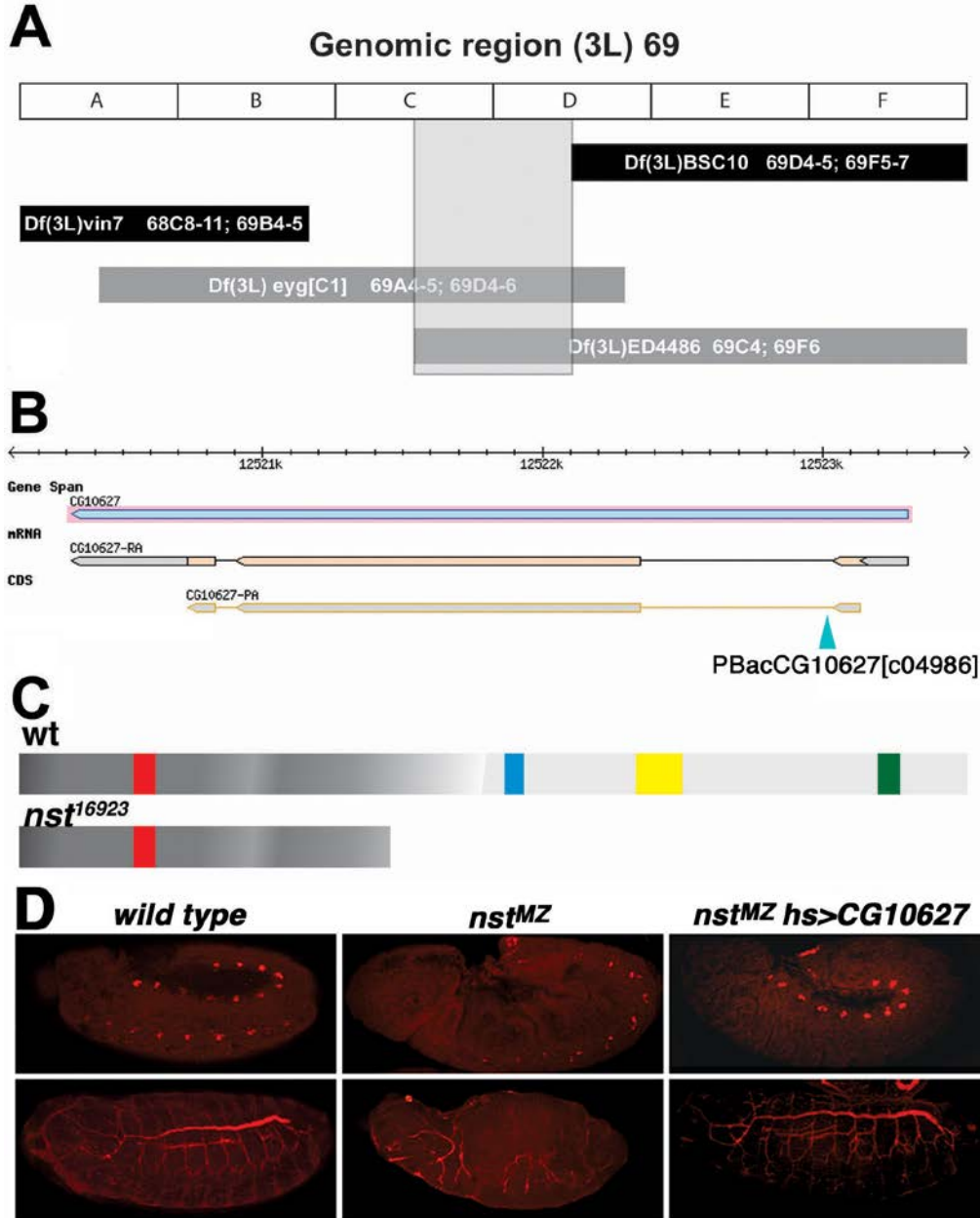


**Fig. S3. Molecular cloning and transgenic rescue of *nst*.** (A) Using chromosomal deletions, the *nst*<sup>16923</sup> mutation was mapped to the genomic region 69C4-D4. The extents of the deletions that did (black bars) or did not (grey bars) complement *nst*<sup>16923</sup> are indicated. (B) A P-element insertion (blue triangle) in the first intron of *CG10627* also does not complement the *nst* mutation. (C) PAGM1 contains four motifs that are all critical for its enzymatic activity: the serine containing catalytic (black), the Mg<sup>2+</sup>-binding (blue), sugar binding (yellow) and phosphate-acceptor (white) motifs. The *nst*<sup>16923</sup> mutation results in a frame shift mutation resulting in a truncated protein product that lacks most of the critical motifs. (D) A genomic construct of *Nst* rescues the mesoderm and tracheal phenotypes. The genotypes of the embryos are indicated and were stained with antibodies detecting Eve or Verm. WT, wild type; *nst*<sup>MZ</sup>, *nst*<sup>16923</sup> MZ; *nst*<sup>MZ</sup> *hs>CG10627*, *hs::CG10627*; *nst*<sup>16923</sup> MZ. See table S3 for quantification.

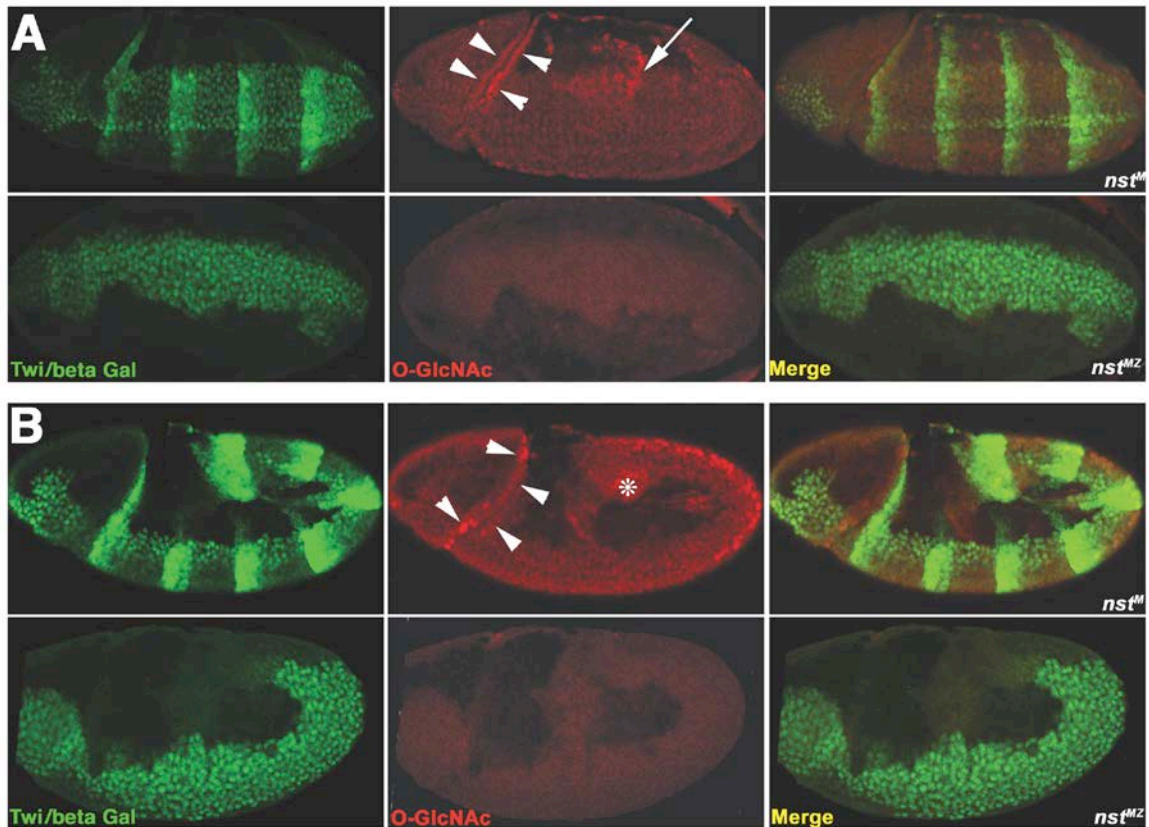


**Fig. S4. O-GlcNAc immunostaining is reduced in  $nst^{16923MZ}$  embryos.** Embryos from  $nst^{16923}$  germ line clone bearing females were obtained by crossing to  $nst^{16923}/TM3[ftz::lacZ]$  males. The presence of the lacZ transgene on the balancer chromosome was detected by anti- $\beta$ -galactosidase (beta-Gal, green stripes) staining. The mesoderm was marked by the presence of Twi (green). O-GlcNAc was detected with the RL2 antibody (red). **(A)** In stage 8  $nst^M$  embryos (ventral view), O-GlcNAc is present in most cells with a pronounced staining of the nuclei. A slight increase in staining can be seen along the cephalic furrow (arrowheads) and neuroectoderm (arrow). Overall O-GlcNAc staining is reduced in  $nst^{16923MZ}$  ( $nst^{MZ}$ ) embryos. **(B)** In stage 9  $nst^M$  embryos (lateral view), O-GlcNAc staining is present in all cells and pronounced staining is observed in the cephalic furrow (arrowheads), the neuroectoderm (arrow), and the posterior midgut (asterisk).

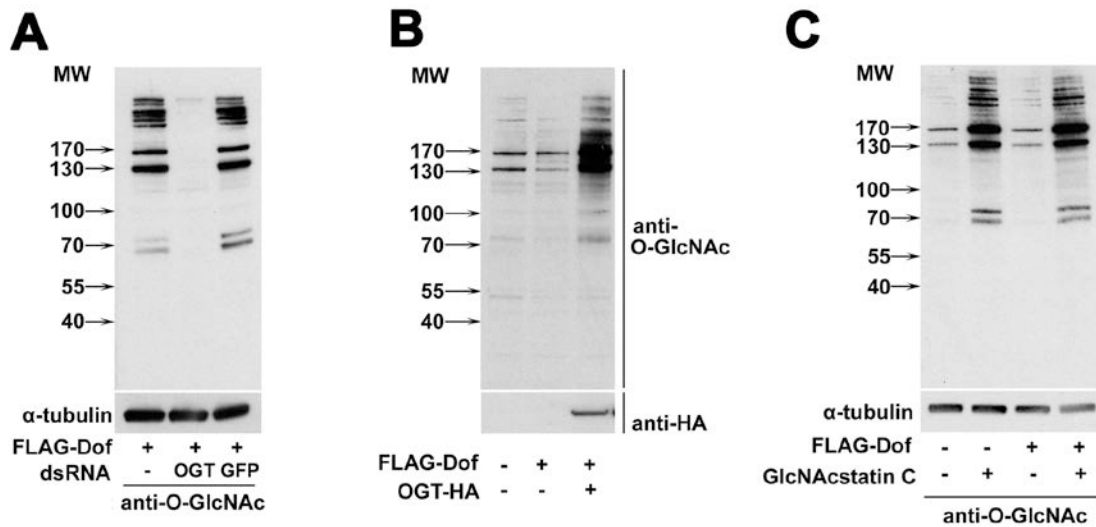


**Fig. S5. Effects on protein O-GlcNAcylation of modulation of OGT and OGA activity in S2 cells.** Lysates of S2 cells were subjected to immunoblot analyses using the RL2 antibody. **(A)** Cells treated with RNAi targeting OGT reduces protein O-GlcNAcylation in S2 cells compared to cells treated with RNAi targeting GFP RNAi as control. Cells transfected with FLAG-Dof were either untreated or treated with dsRNA against OGT or GFP. The samples correspond to the experiment depicted in Figure 5B (last three lanes). **(B)** Overexpression of OGT enhances protein O-GlcNAcylation in S2 cells as assessed by immunoblot with the RL2 antibody recognizing O-GlcNAc (anti-O-GlcNAc). FLAG-Dof was coexpressed with OGT-HA and the samples are derived from the experiment depicted in Figure 5C (last three lanes). **(C)** Treatment of S2 cells with GlcNAcstatin C (1  $\mu$ M) increases protein O-GlcNAcylation. The samples are derived from the experiment depicted in Figure 5D (last four lanes). Molecular weight (MW) of marker proteins is indicated in kD. The data shown are representative of 3 experiments.

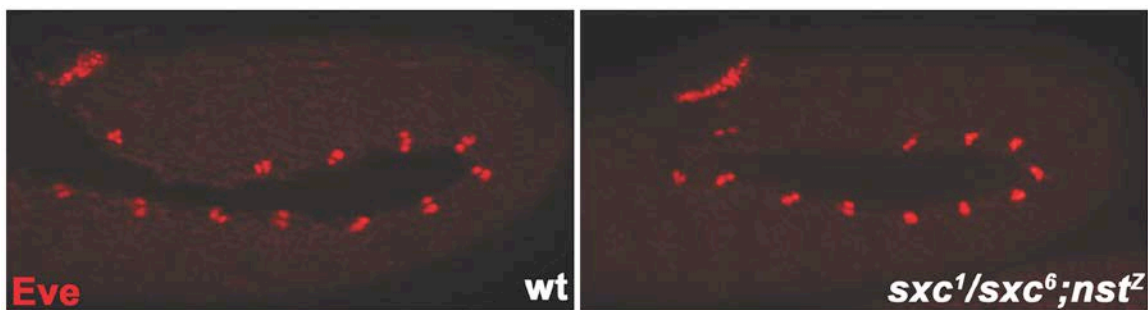


**Fig. S6. Lack of a mesoderm phenotype in *sxc*, *nst* double mutants.** Wild-type (wt) or *sxc<sup>1</sup>/sxc<sup>6</sup>; nst<sup>16923</sup>* zygotic mutants were stained with an antibody against Eve. The wild-type and double mutant embryos have the same number of dorsal mesoderm derivatives, 11 Eve-positive hemisegments.

**Table S1. Genetic interaction between *nst* and *htl*.** The indicated amount of embryos (n) for each genotype was assessed for the number of Eve-positive hemisegments on one body half of the embryo. Shown are the mean values and standard deviation (s.d.) of the respective genotypes. The number of Eve-positive hemisegments for double mutants of *nst*<sup>16923z</sup>, *nst*<sup>04986z</sup> and *Df(3L)4486* with *htl*<sup>YY262</sup> were individually compared to *htl*<sup>YY262</sup> embryos and each pair was significantly different (Student's t-test: P<0.0016, P<0.0003 and P<0.0082 respectively for *nst*<sup>16923z</sup>, *nst*<sup>04986z</sup> and *Df(3L)4486*).

Genotype	Eve-positive hemisegments	s.d.	n
<i>w</i> <sup>1118</sup>	11	0	35
<i>nst</i> <sup>16923MZ</sup>	1.1	2.1	35
<i>htl</i> <sup>YY262</sup>	0.7	1	35
<i>nst</i> <sup>16923z</sup>	11	0	35
<i>nst</i> <sup>04986z</sup>	11	0	35
<i>Df(3L)4486</i>	9.7	1.8	35
<i>htl</i> <sup>YY262</sup> , <i>nst</i> <sup>16923z</sup>	0.06	0.2	35
<i>htl</i> <sup>YY262</sup> , <i>nst</i> <sup>04986z</sup>	0	0	35
<i>htl</i> <sup>YY262</sup> , <i>Df(3L)4486</i>	0.06	0.2	35

**Table S2. Rescue of hatching defects in *nst*<sup>MZ</sup> embryos.** Embryos (n=200) from the indicated crosses were assessed for larva hatching at 29°C.

Cross	Percent hatching
<i>nst</i> <sup>16923</sup> <i>glc</i> X <i>nst</i> <sup>16923</sup> /TM3	15
<i>nst</i> <sup>16923</sup> <i>glc</i> X <i>hs::CG10627;nst</i> <sup>16923</sup> /TM3	78
<i>nst</i> <sup>16923</sup> <i>glc</i> X <i>nst</i> <sup>04986</sup> /TM6	29
<i>nst</i> <sup>16923</sup> <i>glc</i> X <i>hs::CG10627;nst</i> <sup>04986</sup> /TM6	74
<i>nst</i> <sup>16923</sup> <i>glc</i> X <i>Df(3L)4486</i> /TM3	20
<i>nst</i> <sup>16923</sup> <i>glc</i> X <i>hs::CG10627;Df(3L)4486</i> /TM6	68

**Table S3. Measurement of UDP-HexNAc in *mmy* and *nst* embryos.** UDP-HexNAc concentrations were measured for the above genotypes from lysates from embryos collected at the indicated stages. The amount of sugar nucleotide was normalized to total protein concentrations of the lysates. Shown is the range of UDP-HexNAc concentrations for each genotype from two independent experiments. To account for inter-experimental variability, the aminosugar nucleotide concentration for each genotype was measured and compared with lysates from *w<sup>1118</sup>* embryos. *nst<sup>16923z</sup>* – zygotic *nst* mutant; *nst<sup>16923mz</sup>* – maternal-zygotic *nst* mutant; *mmy<sup>JK63z</sup>* – zygotic *mmy* mutant.

Experiment	Stage	Genotype	Range of [UDP-HexNAc] pmol/mg protein
1	9-11	<i>w<sup>1118</sup></i>	6832-8042
		<i>nst<sup>16923z</sup></i>	7545-8579
2	9-11	<i>w<sup>1118</sup></i>	5368-6019
		<i>nst<sup>16923mz</sup></i>	898-956
3	9-11	<i>w<sup>1118</sup></i>	6848-7396
		<i>hs::CG10627;nst<sup>16923mz</sup></i>	5606-5616
4	13-14	<i>w<sup>1118</sup></i>	6057-8309
		<i>nst<sup>16923mz</sup></i>	370-698
5	9-11	<i>w<sup>1118</sup></i>	6975-7756
		<i>mmy<sup>JK63z</sup></i>	3737-4449
6	13-14	<i>w<sup>1118</sup></i>	7038-7868
		<i>mmy<sup>JK63z</sup></i>	561-1135

**Table S4. Tissue-specific rescue of *nst* phenotype.** The indicated amount of embryos (n) for each genotype was assessed for the number of Eve-positive hemisegments on one body half of the embryo. Shown are mean values and standard deviation (s.d.) of the measurements in the respective genotypes. The number of Eve-positive hemisegments for *twi::GAL4/UAS::nst-HA;nst<sup>16923mz</sup>* as compared to *nst<sup>16923mz</sup>* embryos was significantly different (Student's t-test:  $P < 0.0001$ ). Note that the genetics of these crosses with germ line clone producing females only allow half of the embryos to express both *twi::GAL4* and *UAS::nst-HA*. Therefore, the strength of the rescue obtained is an underestimate and represents only about 50% of the real rescue capacity. *UAS::nst<sup>S68A</sup>* encodes an enzymatic dead variant of Nst and does not rescue.

Genotype	Eve-positive hemisegments	s.d.	n
<i>nst<sup>16923mz</sup></i>	1.1	2.1	35
<i>twi::GAL4/UAS::nst-HA/+;nst<sup>16923mz</sup></i>	5.7	4.2	50
<i>twi::GAL4/UAS::nst<sup>S68A</sup>-HA/+;nst<sup>16923mz</sup></i>	1.2	1.7	50

**Table S5. Epistasis experiment of *nst* mutants with  $\lambda$ Htl.** The indicated amount of embryos (n) for each genotype was assessed for the number of Eve-positive hemisegments on one body half of the embryo. Shown are mean values and standard deviation (s.d.) of the respective genotypes.

Genotype	Eve-positive hemisegments	s.d.	n
<i>nst<sup>16923mz</sup></i>	1.1	2.1	35
<i>twi::GAL4/+; UAS::<math>\lambda</math>htl , nst<sup>16923mz</sup></i>	0.7	1.1	35
<i>twi::GAL4/+; UAS::<math>\lambda</math>htl , nst<sup>04986mz</sup></i>	0.5	0.9	35

**Table S6. Suppression of *nst* phenotype by GlcNAcstatin C.** The indicated amount of embryos (n) for each genotype was injected with either the DMSO or GlcNAcstatin C (GC; 0.1 mM in DMSO). The number of Eve-positive hemisegments on one body half of the embryo was scored. Shown are mean values and standard deviations (s.d.) of the respective genotypes. The number of Eve-positive hemisegments for GC-injected *nst<sup>16923mz</sup>* embryos as compared to DMSO-injected *nst<sup>16923mz</sup>* embryos was significantly different (Student's t-test:  $P < 0.0014$ ).

Genotype	Injection	Eve-positive hemisegments	s.d.	n
<i>w<sup>1118</sup></i>	DMSO	11	0	10
	GC	11	0	12
<i>nst<sup>16923mz</sup></i>	DMSO	1.8	1.9	16
	GC	4.8	2.5	19

**Table S7. Overexpression of O-GlcNAc-cycling enzymes in *nst* mutants.** The indicated amount of embryos (n) for each genotype was assessed for the number of Eve-positive hemisegments on one body half of the embryo. Shown are mean values and standard deviations (s.d.) of the respective genotypes. The number of Eve-positive hemisegments for *twi::GAL4/UAS::Ogt-HA;nst<sup>16923mz</sup>* as compared to *nst<sup>16923mz</sup>* embryos was significantly different (Student's t-test: P<0.027). Note that the genetics used in these experiments with germ line clone producing females only allow half of the embryos to express both *twi::GAL4* and the respective UAS transgene. Therefore, the strength of the effect obtained is an underestimate and represents only about 50% of the real capacity.

Genotype	Eve-positive hemisegments	s.d.	n
<i>nst<sup>16923mz</sup></i>	1.1	2.1	35
<i>twi::GAL4/UAS::Oga-HA/+;nst<sup>16923mz</sup></i>	0.9	1.3	35
<i>twi::GAL4/UAS::Ogt-HA/+;nst<sup>16923mz</sup></i>	2.3	2.5	35

**Table S8. Oligonucleotide primers used in this study.** The sequences are presented 5' to 3'.

- 1) Mapping the *nst*<sup>16923</sup> mutation
  - Nst1-For: CTCGGCGGCGGCACCTC
  - Nst1-Rev: TTAAAGCATACGTTCAAAAGTCG
  - Nst2-For: TAACATTCAATAACTCAACTCG
  - Nst2-Rev: AAAAACAACCTTAACTCTCAAAC
  - Nst3-For: TACAAAATAGCGAAGGACATAAAA
  - Nst3-Rev: CCAGGTGGCCAAACTAAGGAGAG
  - Nst4-For: GTTCCGCATCCGTCGTCTCG
  - Nst4-Rev: TCATTAATCAGGGCATCGGTGTCTCG
  - Nst5-For: GTAGTCGGCGCCGAGTCCTC
  - Nst5-Rev: TCCAGCGAAGATAAAAATAGATAG
  - Nst6-For: GGATTGTGCGATGCCGTGAT
  - Nst6-Rev: CCCGCGAGATGTACCCAAAGACC
  - Nst7-For: AAACGCAAATTCCAACATCACAG
  - Nst7-Rev: GCCGAATCTTTTACAACCGCTTAT
  - Nst8-For: TGGTCCAGAGCGAGGTG
  - Nst8-Rev: AACATATCAACATTTTTACATTCC
  
- 2) Cloning *CG10627*
  - CG10627 For: GTCCTACATGTCTCCGCTACTG
  - CG10627 Rev: TCCGTCCGAAAATGAAACTCTAAC
  
- 3) Cloning Nst
  - Nst For: GAAGATCTTCCAGGTGGGCACTGCTGTT
  - Nst Rev: CGGGATCCCGCTACAGGTGGGCACTGCT
  
- 4) Mutagenesis primers Nst[S68A]
  - S68A For: GGAGCAGCAGGTGGCCAAGATCATAAAGGACAAC
  - S68A Rev: GTTGTCTTTTATGATCTTGGCCACCTGCTGCTCC
  
- 5) Cloning OGT and OGA
  - OGT For: GAAGATCTTCATGCATGTTGAACAAACACG
  - OGT Rev: CTTCTAGAAGTACTGCTGAAATGTGGTC
  - OGA For: GAAGATCTTCATGGCAGACGAAGCGGGCAG
  - OGA Rev: CTTCTAGAAGGAAACGGCGACCCATGTAAATACACTT